Laser Ablation of Polyethersulfone Films: The Decomposition of the Chain Structure and the Expansion of Neutral Species Studied by Laser Ionization Mass Spectrometry

Fumio Kokai,*,† Hiroyuki Niino, and Akira Yabe

National Institute of Materials and Chemical Research, Tsukuba, Ibaraki 305-8565, Japan

Received: April 27, 1998; In Final Form: July 13, 1998

Laser ionization time-of-flight (TOF) mass spectrometry has been employed to probe the dynamics of ablation of polyethersulfone (PES) at 266 nm. Neutral products arriving at an ion extraction position, which was 65 mm from a PES film surface, were detected by delaying a post-ionization laser pulse with respect to an ablation laser pulse. At a low fluence of 30 mJ/cm^2, the strongest peak indicating early arrival of C_3H_3 (m/e = 39) was observed at post-ionization delay times of 12−22 μs. As the delay time increased (16−46 μs), some prominent peaks (m/e = 140, 164, 188, 216, 234, 262, 264, 280, 288, 312, 333, and 336) and many weak peaks with m/e up to about 690, which were assigned to direct fragments from PES or secondary products, were observed. Analysis of the products indicates that the decomposition of PES occurs due to both the scission of the polymer chain itself and the cleavage of some phenylene rings in the chain. The average flight velocities of major products ranged from 1.8 × 10^5 cm/s for $C_{15}H_{12}S_2O_5$ (m/e = 336) to 4.1 × 10^5 cm/s for C_3H_3. These products continued to arrive for a period of 6−15 μs, which was over 1200 times the ablation laser pulse length. The distribution, the velocities, and the yields of major products for several higher fluences up to 130 mJ/cm^2 suggest an enhanced decomposition of PES to small fragments in the upper part of a heated surface layer. The arrival profiles of C_3H_3 at various fluences were adequately described by a shifted Maxwell−Boltzmann distribution, indicating collisions among the fragments during an unsteady adiabatic expansion process. We propose a laser-penetration-depth dependent photothermal ablation model.

Introduction

Intense ultraviolet laser pulses can lead to explosive ejection of gaseous and solid fragments at the surfaces of organic polymer films, and then the polymer surfaces are etched with minimal thermal damage. Since the first report of clean etching,[1,2] laser ablation of various polymers has been extensively studied in terms of its application to micropatterning and surface modification and of basic aspects of photochemistry and photophysics in laser−polymer interaction.[3,4]

There have been two mechanisms proposed to interpret polymer ablation by ultraviolet laser pulses: photochemical[5] and photothermal[6,7] ones. In the photochemical mechanism, polymer molecules absorb photons and then directly decompose to gaseous fragments which exert high pressure and lead to an expansion of the irradiated volume. In this mechanism, the decomposition of polymer molecules from electronically excited states plays an important role. On the other hand, in the photothermal mechanism, polymer molecules absorb photons and convert their electronic energies to their vibrational energies at the ground state, and then the temperature of the polymer is raised quickly. The heated polymer decomposes thermally resulting in ablation. In this mechanism, the density of the absorbed energy governs ablation.

A wide range of products, such as atoms, small molecules, high-mass clusters, and solid fragments from polymers, is detected in laser ablation of various polymers. In addition to optical spectroscopic techniques, such as emission spectroscopy, laser-induced fluorescence, and fast photography, mass spectrometry has been extensively applied to characterize neutral and ionic products derived from the decomposition of polymer chains.[8] The distribution of ablation products, ranging from atomic to high-mass cluster species, changed depending on the nature of polymers and laser irradiation conditions such as laser wavelength and fluence. For example, various fragments smaller than the monomer were found in some cases; poly(methyl methacrylate) at 193 nm,[9] 240 nm,[10] and 266 nm,[10] poly(ethylene terephthalate) at 266 nm,[11] and polyimide at 266 nm,[11] and 308 nm.[12] The monomer is predominantly observed in other cases: polystyrene at 193 nm,[13] 248 nm,[14] and 308 nm;[15] poly(α-methylstylene) at 266 nm;[16] and polytetrafluoroethylene at 266 nm,[16] indicating unzipping reactions of polymer chains to produce the monomer. The ablation products from several polymers showed the flight velocities of 10^4−10^6 cm/s.[8,13,14,17] Small degraded species tended to have higher velocities compared to the monomer and high-mass species, for example, C_3 observed in ablation of polycarbonate showed a velocity of 8 × 10^5 cm/s.[17] Both different product distributions observed for different ablation wavelengths[12] and non-Maxwell−Boltzmann (MB) velocity distributions of products[13] supported the photochemical mechanism. In contrast, ablation products similar to those of pyrolysis reaction as seen in unzipping reactions,[11,15] ablation products at 193 nm similar to those in ablation at longer laser wavelengths, and thermal MB velocity distributions of the ablation products[10,15] supported the contribution of the photothermal mechanism. A basic conclusion

* Corresponding author. Telephone: (81) 298-54-4503. Fax: (81) 298-54-4474. E-mail: kokai@nimc.go.jp.

† Permanent address: Institute of Research and Innovation, 1201, Takada, Kashiwa, Chiba 277-0861, Japan. Telephone: (81) 471-44-8811. Fax: (81) 471-44-8939. E-mail: fkokai@iri.or.jp.

10.1021/jp982019i CCC: $15.00
Published on Web 10/01/1998

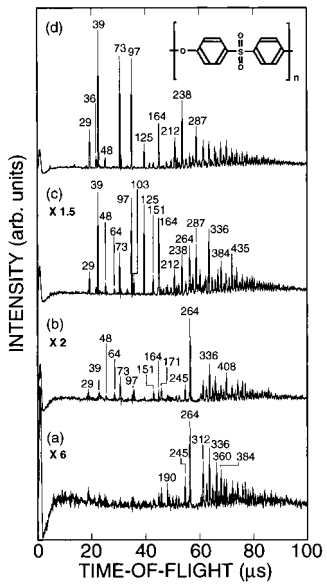

Figure 1. Fluence dependence of ionization laser on the detection of neutral products from laser ablation of PES. TOF mass spectra were measured at a delay time of 40 μs and ArF laser fluences of (a) 10 mJ/cm^2, (b) 20 mJ/cm^2, (c) 40 mJ/cm^2, and (d) 60 mJ/cm^2 for postionization. Ablation was conducted by 266 nm laser pulses at a fluence of 70 mJ/cm^2. The spectra were measured with different sensitivities as indicated by the amplification factors. The masses of major peaks are indicated in amu near each peak. The chemical formula of PES is also shown.

derived from the numerous studies on polymer ablation with ultraviolet lasers is that the contribution of photochemical or photothermal mechanisms and relative importance of the two mechanisms responsible for the decomposition of polymers and ejection of various fragments may strongly depend on the specific system under consideration.

Since laser ablation of polymers includes some time-dependent features, e.g., lengths of ablation laser pulses, lifetimes of electronically excited states, and thermal relaxation times of polymer matrices, analysis of ablation products from a viewpoint of time-dependent fragment ejection is more desirable to understand chemical physics of polymer ablation. In addition, fragments released from a polymer surface are influenced by gas-phase collisions among the fragments.[18,19] Ablation products including pure carbon clusters, which cannot be assigned to direct fragments derived from the chemical structures of polymers, were frequently observed.[8,20,21]

We have shown previously that periodic morphological modification can be developed on the ablated surfaces of polyethersulfone (PES) derivatives.[22,23] It was considered of interest to investigate the decomposition mechanisms of these polymers. In this paper we therefore applied laser ionization time-of-flight (TOF) mass spectrometry to laser ablation of a PES film (poly(1,4-oxyphenylenesulfone-1,4-phenylene)) at 266 nm with a nanosecond pulse duration. Compared to the chemical structures of three prototypical polymers—poly(methyl methacrylate); polyimide; and poly(ethylene terephthalate), frequently used in ablation studies—PES, whose monomer unit is composed of two phenylene groups, a sulfone group, and an ether oxygen,[22] has a unique structure possessing carbon−carbon bonds limited within the phenylene rings (Figure 1). By delaying an ionization laser pulse with respect to an ablation laser pulse, time-resolved TOF mass spectra were measured for the neutral products ejected from the PES film at fluences of 30−130 mJ/cm^2, which are near the threshold of ablation. Major products were identified and their arrival time distributions were compared and analyzed as a function of laser fluence. Dynamical aspects in the decomposition of the chain structure, the ejection of various fragments, and their expansion accompanied by gas-phase collisions are discussed. We propose a laser-penetration-depth dependent photothermal model for ablation of PES.

Experimental Section

Sample. Samples of PES films (Mitsui Toatu Chemicals, TALPA-1000LC, 70 μm thick) were cleaned ultrasonically with ethanol before use. PES is a heat-resisting amorphous polymer having a glass transition point of 230 °C, and shows intense absorption in the ultraviolet region. The absorption coefficient of a spun-on PES film (67 nm thick) is 8.2×10^5 cm^{-1} at 266 nm.[22]

Apparatus. Laser ionization TOF mass spectrometry applied here is almost the same as that of previous works.[8,24] Briefly, laser ablation of PES was performed in a vacuum chamber combined with a TOF mass spectrometer (Jordan), pumping down to $<4 \times 10^{-5}$ Pa with two turbomolecular pumps. A sheet of the PES film (10 mm × 10 mm) was placed at a distance of 60 mm from the repeller of the TOF mass spectrometer, and rotated at 6 rpm using a stepping motor. The fourth harmonic (4−5 ns pulse width) from a Nd:YAG laser (Quanta-Ray GCR-130), operated at a repetition rate of 1 Hz, was focused with an incident angle of ∼45° on the PES film through a 300 mm focal length lens and an iris down to 1 mm spot size. The spot size was determined from the burn pattern on a colored paper. The energy of the laser pulse was measured with a Gentec ED-200 joulemeter. Using optical filters, the laser fluence at the film surface was set to be 30−130 mJ/cm^2, which was close to the threshold of ablation of PES. At these fluences, most of the volatile products were thought to be neutral species. The 193 nm pulses from an ArF excimer laser (Lumonics EX-742; 12 ns pulse width) produced at variable delays (<50 μs) relative to the 266 nm ablation laser pulses were used to postionize neutral species arrived between the repeller and the extraction grid of the TOF mass spectrometer. The beam size of the ArF laser was set to be 1 mm in diameter through an iris. The flight length of ejected neutral species from the film surface to the ionization position (the center of the ArF laser beam) was 65 mm. To examine the influences of fragmentation during the ionization, the fluences of the ArF laser were varied from 10 to 60 mJ/cm^2. After ionization, the positive ions were detected with a dual microchannel plate (Galileo). The TOF signals were accumulated 40 times by a digital oscilloscope (LeCroy 9310AL) to improve the signal-to-noise ratio. The experimental uncertainties in the conversion of the time, at which a mass peak appears, into the masses were ±1 at 200 amu and ±2 at 400 amu, respectively.

Results and Discussion

Photofragmentation during Postionization. We first describe the influence of the fluence of a post-ionization laser pulse on the detection of neutral products from ablation of PES. Figure 1 shows TOF mass spectra of the products measured at a delay time of 40 μs by using four fluences of 10, 20, 40, and 60 mJ/cm^2 for postionization. Ablation of a PES film was performed by 266 nm laser light at a fluence of 70 mJ/cm^2. Although signal-to-noise ratios were lost, we attempted to ionize the neutral species using a fluence as low as 10 mJ/cm^2 to minimize fragmentation during the ionization. As seen in Figures 1b−d, the increase in the ArF laser fluene leads to dramatical change in the intensities of the peaks at 29, 39, 73,

TABLE 1: Major Ions Formed by Photofragmentation of the Ablation Products of PES

m/e	possible species
29	$C_2H_5^+$, CHO^+
36	C_3^+
39	$C_3H_3^+$
48	SO^+
64	SO_2^+
73	$C_4H_9O^+$
97	$C_6H_9O^+$
103	$C_3H_3SO_2^+$
125	$C_6H_5SO^+$
151	$C_8H_6SO^+$
164	$C_9H_5SO^+$

97,125 and 164 amu in the lower TOF region (20−50 μs), which are due to the fragments formed during the ionization. The intensity distribution in the higher TOF region (50−90 μs) also varies significantly depending on the ionization laser fluence. In contrast, as seen in Figure 1a, the intensities of the major peaks at 245, 264, 312, 336, and 384 amu due to parent molecular ions are enhanced with decreasing the ionization laser fluence.

Although avoiding the fragmentation during ionization would be nearly impossible in the present experimental approach, we believe that the mass peaks in Figure 1a represent arrival products more directly. Many peaks at 50−90 μs in Figure 1a, including the major peaks at 245, 264, 312, 336, and 384 amu, are assigned to the ablation products with higher masses than monomer ethersulfone (ES, m/e = 232), generated from the decomposition of PES upon 266 nm laser irradiation. The decomposition process of PES is discussed later. Like the polyatomic aromatic molecules with ionization potentials of 7−10 eV,[25] these ablation products are thought to require two photons from an ArF laser for ionization (193 nm corresponds to 6.4 eV). Table 1 shows tentative assignments for the fragment peaks observed in Figures 1b−d. The fragments peculiar to the chemical structure of PES such as SO (m/e = 49), SO_2 (m/e = 64), and C_6H_4SO (m/e = 125) are included. We note here that the various fragments in Table 1 are derived from a multiphoton decomposition process for some ablation products of PES. To minimize fragmentation during postionization, all the data shown below were obtained at a fluence as low as 10 mJ/cm^2.

Assignments of Ablation Products and Their Arrival Behaviors. Figure 2 shows a series of TOF mass spectra of ablation products observed at delay times of 12−46 μs following the ablation laser at a fluence of 30 mJ/cm^2. A significant change in the intensity distribution in the mass spectra is observed depending on the delay time of postionization. This indicates that the nature and the amount of arrival species change with the time after laser irradiation of a PES surface. At earlier arrival times, as seen in the spectra at delay times of 12−22 μs, the strongest peak is observed at 39 amu. As the delay time increases, some prominent peaks (m/e = 140, 164, 188, 216, 234, 262, 264, 280, 288, 312, 333, and 336) and many weak peaks with m/e up to about 690 (corresponding to 90 μs) appear in the higher TOF region.

Possible assignments for primary peaks observed in the TOF mass spectra are listed in Table 2. The peaks at 140 and 216 amu are assigned to $C_6H_4SO_2$ and $C_{12}H_8SO_2$, respectively, possessing phenylene and sulfone groups. These two products reflect the partial chemical structure of monomer ES and can be viewed as direct fragments from PES. In contrast, other peaks shown in Table 2, including the strongest peak at 39 amu (C_3H_3), cannot be assigned to direct fragments. These products

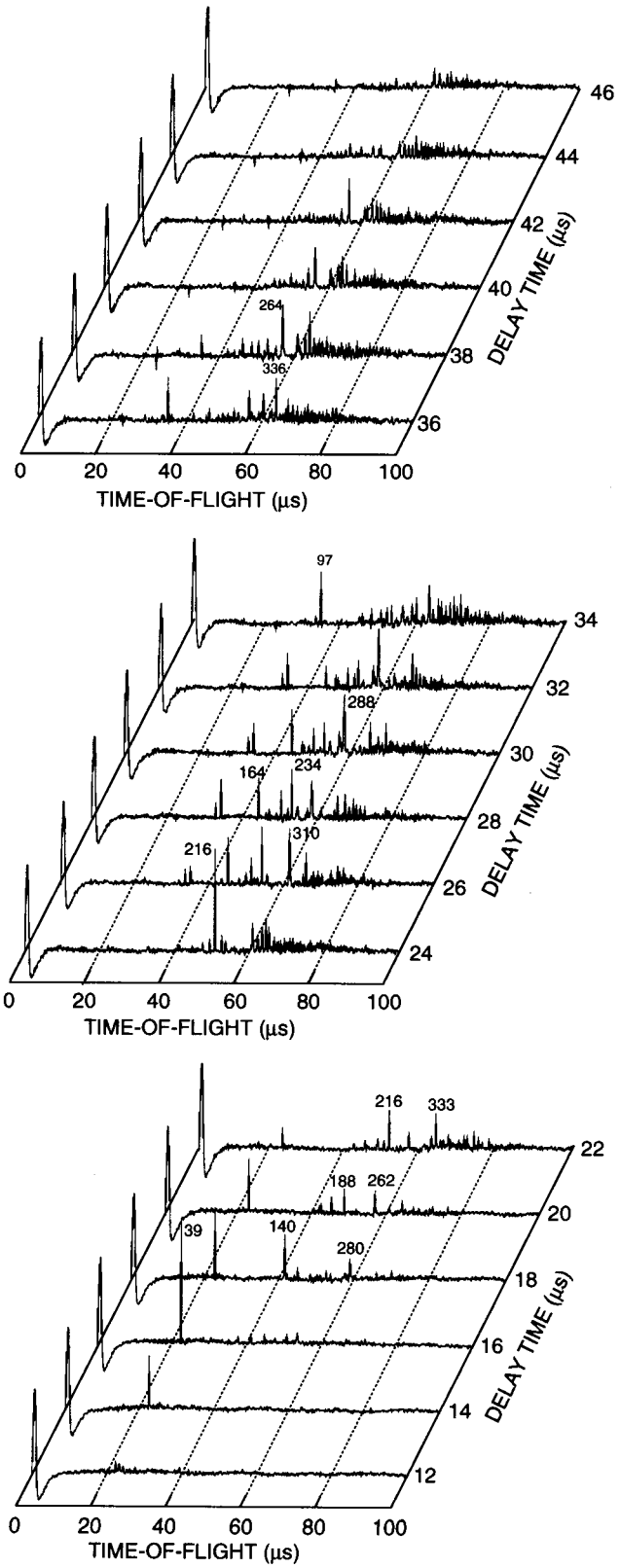

Figure 2. TOF mass spectra of the products from laser ablation of PES measured at an ionization laser fluence of 10 mJ/cm^2 and delay times of 12−46 μs. Ablation was conducted at a fluence of 30 mJ/cm^2. The masses of major peaks are indicated in amu near each peak.

are probably due to secondary products via collision-induced reactions in gas phase near the film surface, e.g., the attachment of hydrogen or the recombination among the fragments. Similarly, in laser ablation of several polymers,[8,10,12,14,20,21] secondary products were reported to exist. In addition to the

TABLE 2: Major Ions Observed in TOF Mass Spectra for Laser Ablation of PES

m/e	possible species[a]
39	$C_3H_3^+$
97	$C_6H_9O^+$
140	$C_6H_4SO_2^+$
164	$C_9H_8SO^+(C_6H_4-SO-C_3H_3^+)$
188	$C_6H_4S_2O_3^+(SO_2-C_6H_4-SO^+)$
216	$C_{12}H_8SO_2^+(C_6H_4-SO_2-C_6H_4^+)$
234	$C_{12}H_{10}SO_3^+(C_6H_5-SO_2-C_6H_4-OH^+)$
262	$C_{14}H_{14}SO_3^+(C_2H_5-C_6H_4-SO_2-C_6H_4-OH^+)$
264	$C_{13}H_{12}SO_4^+(CH_3O-C_6H_4-SO_2-C_6H_4-OH^+)$
280	$C_{12}H_8S_2O_4^+(C_6H_4-SO_2-C_6H_4-SO_2^+)$
288	$C_{15}H_{12}SO_4^+(C_6H_4-SO_2-C_6H_4-SO_2^+)$
312	$C_{18}H_{14}SO_3^+(C_3H_3-O-C_6H_4-SO_2-C_6H_4-C_3H_3^+)$
333	$C_{16}H_{13}S_2O_4^+(SO-C_3H_3-O-C_6H_4-SO_2-C_6H_4-CH_2^+)$
336	$C_{15}H_{12}S_2O_5^+(SO-C_3H_3-O-C_6H_4-SO_2-C_6H_4-OH^+)$

[a] The possible structure is given in parentheses in some cases.

contribution of the collision-induced reactions among the fragments, another possible explanation of the formation of the products is laser-induced surface modification such as a rearrangement of an original PES structure. XPS and FT-IR studies on the ablated surfaces of polyimide and poly(ethylene terephthalate) indicated that the changes in the atomic composition and the chemical bonding state occurred at laser-irradiated polymer surfaces.[26,27] Even after one pulse irradiation, the feature of the ablated surface differed from that of a fresh polymer surface. In the present study, ion signals were accumulated 40 laser shots for the measurement of a TOF mass spectrum. In addition to the prominent peaks, many weak peaks exist in the higher TOF region of 50−90 μs. The molecular weight distribution of PES molecules and their amorphous structures in the film also seem to affect the distribution of the peaks.

A peak assigned to the product of ES monomer with two hydrogen atoms attached is seen at 234 amu in Figure 2. However, unlike the ablation of some polymers, such as polystylene governed by an unzipping reaction, where a very strong peak of the monomer was observed,[13−15] the ablation of PES is not thought to proceed by the unzipping reaction. The peaks indicating exclusive ejection of the dimmer or trimmer are also not present. Instead, the product distribution including C_3H_3 indicates that the decomposition of PES is due to both the scission of the polymer chain itself, i.e., in the C−S and C−O bonds, and the cleavage of some of the phenylene rings in the chain.

A significant change in the intensity of each peak depending on the delay time of postionization in Figure 2 indicates that the arrival dynamics of neutral species vary from species to species. The intensities of prominent peaks at 39, 140, 164, 216, 234, 264, 288, and 336 amu are plotted as a function of arrival time (delay time of postionization) in Figure 3. Each product shows a flight distribution with the maximum intensity at a different arrival time. The average flight velocities, estimated from the arrival time showing the maximum intensity and a flight length of 65 mm, range from 1.8×10^5 cm/s for $C_{15}H_{12}S_2O_5$ (m/e = 336) to 4.1×10^5 cm/s for C_3H_3 (m/e = 39).[28] Fast photographic images for ablation of poly(methyl methacrylate) at 248 nm[29,30] and polyimide at 248 and 308 nm[31] in air showed that a shock wave with small atomic and molecular fragments appeared and subsequently solid fragments started to leave the film surface (50−500 ns after ablation laser irradiation). This time-dependent ejection of the fragments suggests that a slightly delayed departure of the high-mass products, such as $C_{15}H_{12}SO_4$ (m/e = 288) and $C_{15}H_{12}S_2O_5$ (m/e = 336), occurs in the present study. However, the profiles of the high-mass products are seen in a period of 10−50 μs in Figure 3; the changes in the average velocities are at most 3% estimated from a delay of 500 ns.

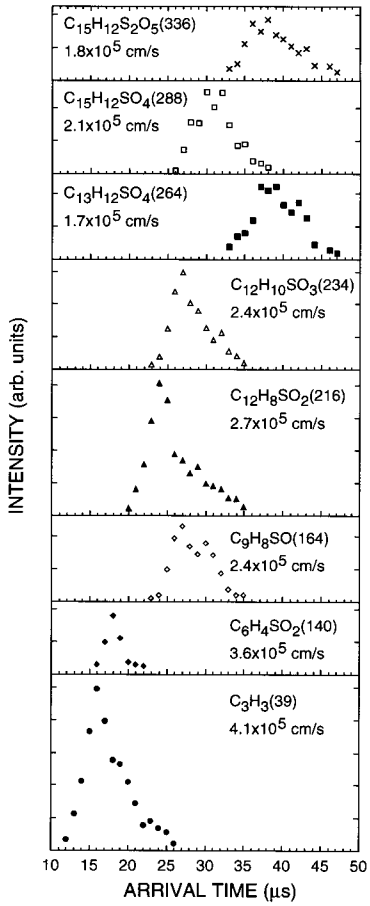

Figure 3. Arrival profiles of some major products (m/e = 39, 140, 164, 216, 234, 264, 288, 336) observed for laser ablation of PES at 30 mJ/cm^2. The mass in a parenthesis and the average flight velocity are indicated for each product. The average translational energies are calculated to be 3.3, 9.3, 4.9, 8.1, 6.9, 3.9, 6.5, and 5.6 eV for C_3H_3, $C_6H_4SO_2$, C_9H_8SO, $C_{12}H_8SO_2$, $C_{12}H_{10}SO_3$, $C_{13}H_{12}SO_4$, $C_{15}H_{12}SO_4$, and $C_{15}H_{12}S_2O_5$, respectively.

In Figure 3, there is a tendency that higher mass products show lower flight velocities, which was also observed for ablation of other polymers studied by mass spectrometry.[8,11,17] However, we note that the average velocities estimated here do not necessarily decrease with the order of the mass. It is also worth noting that the ablation products continue to arrive for a period of 6−15 μs, which is over 1200 times the ablation laser pulse length. This indicates the formation process of each product with various velocities. For example, C_3H_3 with velocities of $(2.5-5.4) \times 10^5$ cm/s are formed. Fragment arrival processes continuing for over several microseconds in ultraviolet laser ablation of polymers were also observed in earlier work.[11,17] The arrival profiles observed are thought to be determined by translational energy distributions of the fragments received when leaving the surface and gas-phase collisions among the fragments. In the ablation of PES, as mentioned later, we consider that the translational energies of the fragments result from the temperature at which thermal decomposition of the chain of PES takes places depending on a laser-penetration-depth. The arrival profiles of the early arrivals C_3H_3 and $C_6H_4SO_2$ show distributions with narrower widths than those of other later arriving products (see also Figure 5). This can be explained by the influence of collisions among the fragments in a Knudsen

layer (KL).[18,19] Enhanced collisions likely occur for early arrival products because of their higher abundances than those of later arriving products.

Additionally, some of the average translational energies (3.3−9.3 eV) calculated from the average velocities of major ablation products exceed the photon energy of 266 nm laser light (4.7 eV). Multiphoton absorption like a proposed cyclic multiphotonic absorption process[32] during an ablation laser pulse may contribute to the laser absorption of PES molecules followed by a rapid relaxation of electronic energy to thermal energy. In addition to the multiphoton process, there may be other sources of the translational energy, chemical energy from the decomposition of PES, and collisional energy in the plume during expansion of ablation products.

Influence of Laser Fluence on the Flight Velocities and the Yields of Ablation Products. To examine the decomposition of PES and the subsequent ejection of fragments in detail, TOF mass spectra were measured at several higher laser fluences up to 130 mJ/cm^2. The nature and amount of early arrival species such as C_3H_3 changed significantly with an increase of the fluence. As a representative example, a series of TOF mass spectra observed at 100 mJ/cm^2 is shown in Figure 4. The strongest peak at 39 amu ($C_3H_3^+$) appears at delay times of 8−16 μs, indicating an earlier arrival of C_3H_3 than that at 30 mJ/cm^2. In addition to the $C_3H_3^+$ peak, the peaks due to low-mass products, which are not strong peaks, appear at 36, 44, 73, and 97 amu (see also Figure 8). These peaks at 36, 44, 73, and 97 amu can be assigned to C_3^+, $C_2H_4O^+$, $C_4H_9O^+$, and $C_6H_9O^+$, respectively. However, some peaks at 140, 188, and 216 amu observed prominently at 30 mJ/cm^2 are not major peaks at 100 mJ/cm^2. These findings indicate an enhanced decomposition of PES to smaller fragments at 100 mJ/cm^2. Unlike Figure 1b−d, there is no clear peak showing the presence of small products containing sulfur such as SO and SO_2. This is probably not an indication of the absence of these fragments but due to the detection problem like a low-ionization cross section. On the other hand, at delay times greater than approximately 24 μs, TOF mass spectra containing prominent peaks at 164, 234, 264, 288, and 336 amu, which are analogous to those at 30 mJ/cm^2, are seen in Figure 4. The origins of these high-mass products are probably different from those of the small products such as C_3H_3 whose relative yields and velocities are sensitive to laser fluence. It is interesting to note that TOF mass spectra at delay times of >24 μs measured under other fluence conditions showed a similar intensity distribution, although the absolute abundance of the products varied depending on the fluence (Figure 7a).

The intensities of the peaks at 36, 39, 44, 73, 97, 164, 234, 264, 288, and 336 amu as seen in Figure 4 are plotted as a function of arrival time in Figure 5. The average velocities of early arrival low-mass products of C_3 (m/e = 36), C_3H_3 (m/e = 39), C_2H_4O (m/e = 44), C_4H_9O (m/e = 73), and C_6H_9O (m/e = 97) are calculated to be (5.4−8.1) × 10^5 cm/s. These low-mass products have higher velocities than the velocity of C_3H_3 at 30 mJ/cm^2 (4.1 × 10^5 cm/s). Alternatively, later arrival products of C_9H_8SO (m/e = 164), $C_{12}H_{10}SO_3$ (m/e = 234), $C_{13}H_{12}SO_4$ (m/e = 264), $C_{15}H_{12}SO_4$ (m/e = 288), and $C_{15}H_{12}S_2O_5$ (m/e = 336) have profiles with peak positions similar to those at 30 mJ/cm^2. As seen in Figure 3, the early arrival products show narrower profiles compared to those of the later arrival products.

Figure 6 shows the fluence dependence of the average velocities of four products, C_3H_3 (m/e = 39), C_2H_4O (m/e = 44), $C_{12}H_8SO_2$ (m/e = 216), and $C_{12}H_{10}SO_3$ (m/e = 234), which

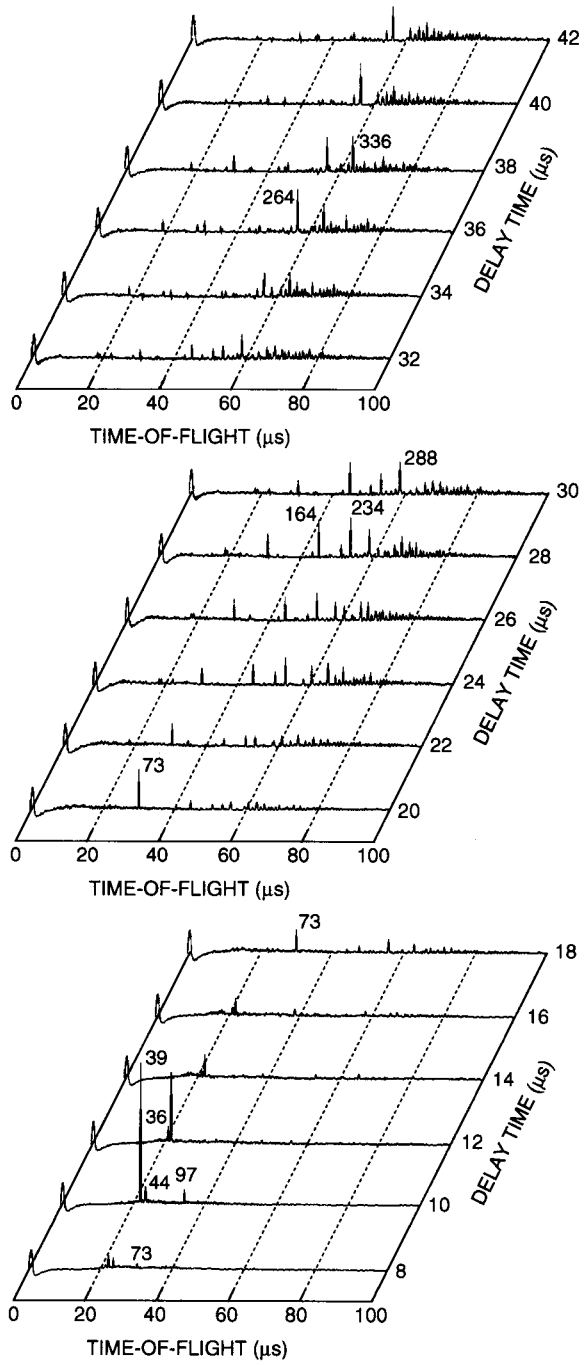

Figure 4. TOF mass spectra for an ablation laser fluence of 100 mJ/cm^2 measured at an ionization laser fluence of 10 mJ/cm^2 and delay times of 8−42 μs. The masses of major peaks are indicated in amu near each peak.

seems to be important to understand the ablation process of PES in the fluence region of 30−130 mJ/cm^2. The velocities of C_3H_3 and C_2H_4O significantly increase with an increase of laser fluence. The velocities of early arrival products of C_3 (m/e = 36), C_4H_9O (m/e = 73), and C_6H_9O (m/e = 97) also similarly increase. In addition, the velocity of $C_{12}H_8SO_2$, which is a predominant species at lower fluences, slightly increases with increasing fluence. The velocities of predominant products at lower fluences, including $C_6H_4SO_2$ (m/e = 140) and $C_6H_4S_2O_3$ (m/e = 188), also analogously increase. On the other hand, the velocity of $C_{12}H_{10}SO_3$ is found to be almost constant when the fluence is changed. The later arrival products, such as C_9H_8SO (m/e = 164), $C_{13}H_{12}SO_4$ (m/e = 264), and $C_{15}H_{12}SO_4$ (m/e = 288), also showed that the velocities were not changed by

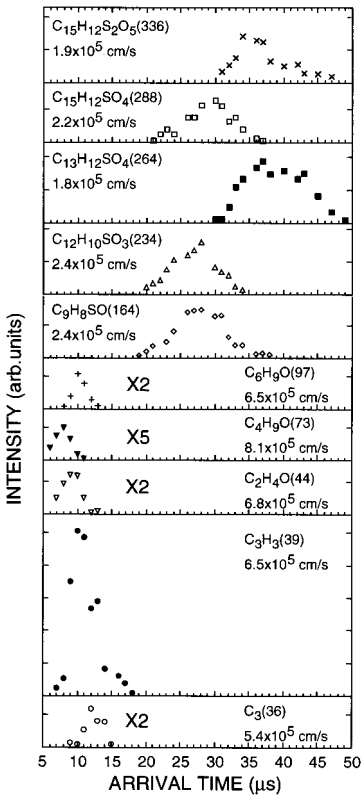

Figure 5. Arrival profiles of some major products (m/e = 36, 39, 44, 73, 97, 164, 234, 264, 288, 336) at 100 mJ/cm^2. The mass in a parenthesis and the average flight velocity are indicated for each product. The profiles were made by mass spectra measured with different sensitivities as indicated by the amplification factors. The average translational energies are calculated to be 5.4, 8.5, 10.5, 24.6, 21.1, 4.9, 6.9, 4.4, 7.2, and 6.2 eV for C_3, C_3H_3, C_2H_4O, C_4H_9O, C_6H_9O, C_2H_4O, C_9H_8SO, $C_{12}H_{10}SO_3$, $C_{13}H_{12}SO_4$, $C_{15}H_{12}SO_4$, and $C_{15}H_{12}S_2O_5$, respectively.

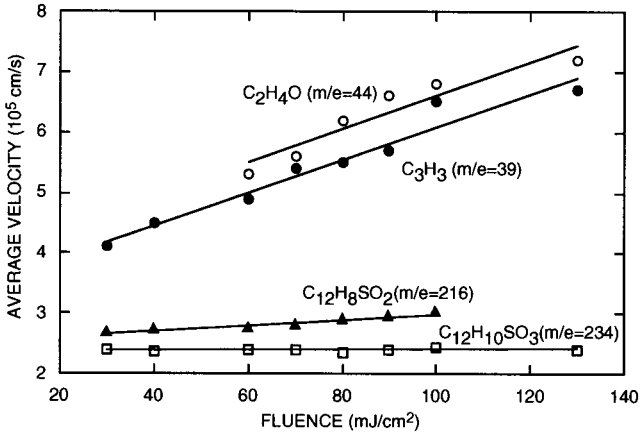

Figure 6. Fluence dependence of the average velocities of C_3H_3 (m/e = 39), C_2H_4O (m/e = 44), $C_{12}H_8SO_2$ (m/e = 216), and $C_{12}H_{10}SO_3$ (m/e = 234). The linear lines are least-mean-squares fits for each plot.

fluence. The flight velocities of C_3H_3 and C_2H_4O ranging from 4.1 × 10^5 to 7.2 × 10^5 cm/s obtained here are equivalent to those of small products observed in ablation of several polymers, for example, C_3 (8 × 10^5 cm/s) in ablation of polycarbonate at 266 nm,[17] CN (6.5 × 10^5 cm/s) in the ablation of polyimide at 248 nm,[33] and CH, C_2, and CN (2−5 × 10^5 cm/s) in the ablation of poly(methyl methacrylate) at 193 nm.[34]

The fluence dependence of the velocities of the four products would be explained in terms of the decomposition of the heated surface layer which has a temperature gradient along its depth because of the penetration depth of laser light. The early arrival products such as C_3H_3, C_2H_4O, and $C_{12}H_8SO_2$, whose velocities vary with fluence, originate from the upper part of the surface layer where its temperature depends directly on the laser fluence. In contrast, the later arrival products such as $C_{12}H_{10}SO_3$, whose velocities are not sensitive to the fluence, originate from the lower part of the surface layer. The increase in the flight velocities of C_3H_3, C_2H_4O, and $C_{12}H_8SO_2$ with increasing laser fluence is consistent with a photothermal mechanism, in which the density of the absorbed energy by the surface of a polymer film plays an important role rather than the energy of an excited electronic state. Recent molecular dynamics simulation of laser ablation of organic solids by Zhigilei et al.[35] indicates that pressure-driven ablation, due to thermal energy of translational motions of molecules, leads to different ejection conditions for molecules depending on their original depths in the solid. Moreover, their simulation suggests that the molecules originally at the top of the solid tend to get accelerated during the plume expansion and those at the bottom get decelerated.

Arrival yields of ablation products can be estimated by the areas surrounded by the experimental points in Figures 3 and 5. The estimated arrival yields of the four important products, C_3H_3, C_2H_4O, $C_{12}H_8SO_2$, and $C_{12}H_{10}SO_3$, are shown as a function of fluence in Figure 7a. The fluence dependence of each yield is found to vary product to product. In addition to the case of the velocity mentioned above, we consider that C_3H_3, C_2H_4O, and $C_{12}H_8SO_2$ originate from the upper surface layer. In the lower fluence region of 30−70 mJ/cm^2, the yields of C_3H_3 and $C_{12}H_8SO_2$ increase with increasing fluence. These increases can be interpreted by both a rise in the temperature of the upper surface layer and an increase in the volume of the layer which decomposes into fragments. The steeper increase in the yield of C_3H_3 than that of $C_{12}H_8SO_2$ at 30−60 mJ/cm^2, the decrease in the yield of $C_{12}H_8SO_2$ with increasing fluence at 60−100 mJ/cm^2, and the appearance of C_2H_4O at 60−130 mJ/cm^2 probably result from an enhancement of the decomposition of PES into smaller fragments due to temperature elevation. The slight increase in the yield of $C_{12}H_{10}SO_3$ at 30−70 mJ/cm^2, which is regarded as the product originated from the lower surface layer, may be explained by the increase in the layer volume decomposed. From the yields of C_3H_3, $C_{12}H_8SO_2$, and $C_{12}H_{10}SO_3$ at 30−70 mJ/cm^2, a threshold fluence for the ejection of neutral species is determined to be 10−20 mJ/cm^2.

We tentatively plot the yields of C_3H_3 and $C_{12}H_8SO_2$ obtained in the lower fluence region against the reciprocal of the fluence in Figure 7b. The yields plotted on a log scale show nearly exponential dependence on the reciprocal of the fluence. If the fluence is proportional to the temperature, the dependence observed here indicates that the decomposition of PES and subsequent fragment ejection obeys an Arrehnius-type law, indicating a significant role of a thermally activated process.[15,35] The difference in the slopes of C_3H_3 and $C_{12}H_8SO_2$ may be ascribed to that in their activation energies. We should note that the yields of ablation products always have to be directly proportional to the rate constants showing Arrehenius behavior. The type of bonds, functional groups, and their arrangements strongly affects decomposition characteristics. We also note that the heat capacity relating to the conversion of laser energy into heat may be a strong function of temperature.

The decrease in the yields of all products at higher fluences in Figure 7a may be due to several reasons, e.g., the absorption of laser light by ablated fragments and conversion of neutral fragments into ionic species through laser and/or electron-impact ionization. Figure 8 shows TOF mass spectra for ablation laser

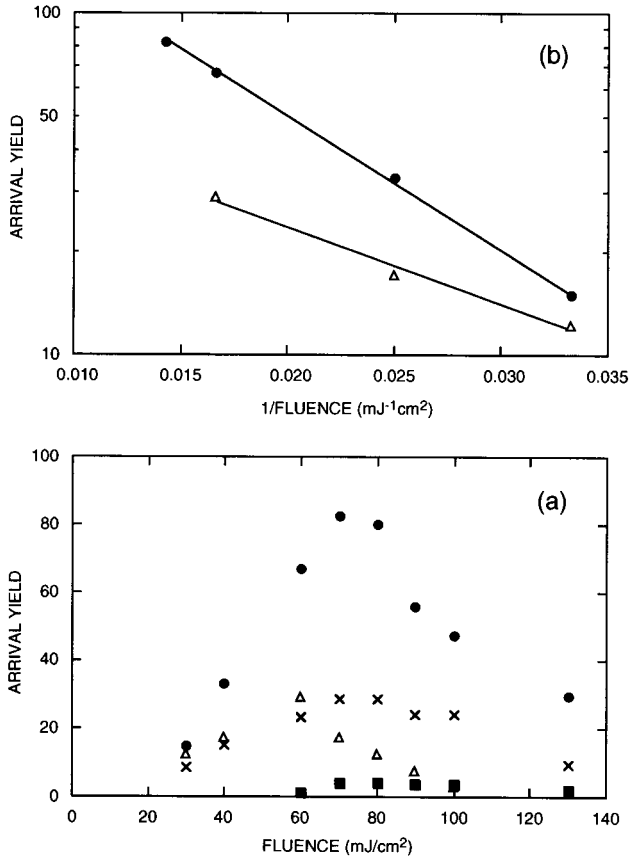

Figure 7. Arrival yields of C_3H_3 (●), C_2H_4O (■), $C_{12}H_8SO_2$ (△), and $C_{12}H_{10}SO_3$ (×); (a) plot as a function of laser fluence, (b) plot for C_3H_3 and $C_{12}H_8SO_2$ as a function of the reciprocal of laser fluence at 30−70 mJ/cm^2. The linear lines are least-mean-squares fits for each plot.

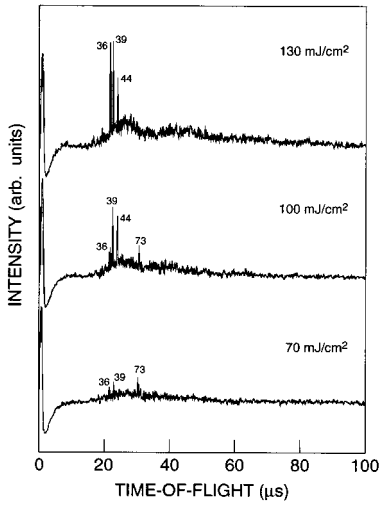

Figure 8. TOF mass spectra of the products from laser ablation of PES detected at a delay time of 8 μs. Ablation laser fluence is 70, 100, and 130 mJ/cm^2. The sharp and broad background signals are assigned to neutral and ionic species, respectively. The masses of the peaks due neutral species are indicated in amu near each peak.

fluences of 70, 100, and 130 mJ/cm^2 measured at a delay time of 8 μs. In addition to sharp peaks at 36, 39, 44, and 73 amu due to early arrival neutral products, the broad signals, whose intensities increase with an increase of fluence, are observed. These broad signals are attributed to ionic species directly produced by laser ablation.

Expansion of Ablation Products. The arrival profiles of C_3H_3 obtained at several fluences of 30−130 mJ/cm^2 were

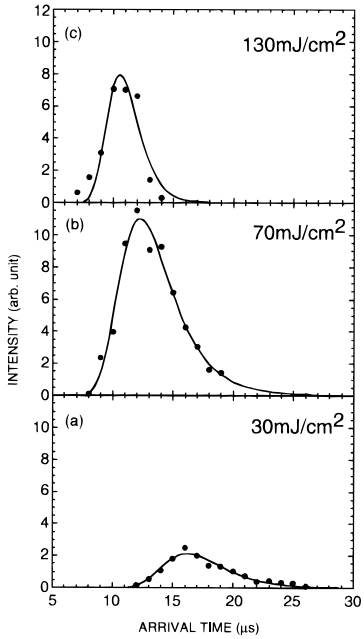

Figure 9. Arrival profiles of C_3H_3 at fluence of (a) 30, (b) 70, and (c) 130 mJ/cm^2. The solid lines represent fits to shifted MB distributions with center-of-mass velocities of (a) 3.6×10^5, (b) 4.6×10^5, and (c) 5.8×10^5 cm/s and KL temperatures of (a) 1900, (b) 4660, and (c) 2620 K.

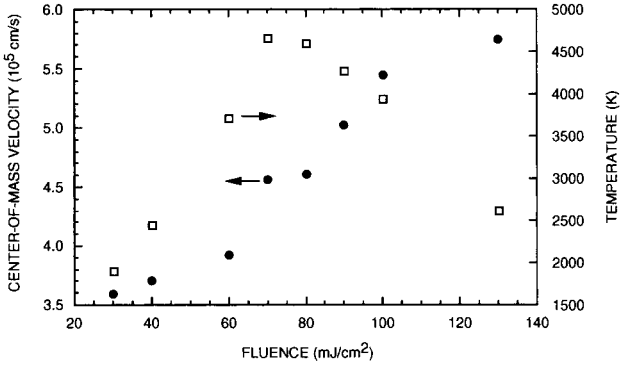

Figure 10. Fluence dependence of the center-of-mass velocity and the KL temperature of C_3H_3 obtained by the curve fitting using a shifted MB distribution.

analyzed by curve fitting using a Maxwell−Boltzmann (MB) distribution and a shifted MB distribution.[18,19] All of the profiles observed were found to be narrower than a MB distribution and were adequately described by a shifted MB distribution defined with a center-of-mass velocity and a KL temperature. This indicates the formation of a KL layer near the surface of a PES film and an unsteady adiabatic expansion, in which collision processes among fragments shift the flight distributions along the direction normal to the surface.[18,19] Figure 9 shows typical arrival profiles at 30, 70, and 130 mJ/cm^2, together with fitted curves using a shifted MB distribution. Although the peak position and the width of the profiles are different at the three fluences, a shifted MB distribution provides a good fit to each profile. Figure 10 shows plots of the center-of-mass velocity and the KL temperature obtained from the curve fitting as a function of fluence. The center-of-mass velocity increases with the fluence over the range of 30−130 mJ/cm^2, similar to the change in the average velocities in Figure 6. Alternatively, the KL temperature rises with increasing fluence up to 70 mJ/cm^2 and goes down as the fluence increases further. The behaviors of the center-of-mass velocity and the KL temperature can be

attributed to the temperature elevation and distribution in a laser irradiated surface layer and the increase in the number of the collision among the fragments with increasing fluence. When the fluence is higher than 70 mJ/cm^2, collision processes during the expansion, leading to the reduction in the KL temperature, most likely prevail the effect of the temperature distribution in the laser irradiated surface layer, which result in the ejection of fragments with a certain range of the KL temperature.

Mechanism of Laser Ablation of PES. The studies on photochemical decomposition of a series of aromatic sulfones in solution were performed using a cw, low-intensity light source.[37,38] The breakage of a carbon−sulfur bond dominantly occurred and yielded aryl radicals. Biphenyl and benzenesulfonic acid were observed as the reaction products of biphenyl sulfone in benzene at 254 nm.[39] In the commercial polysulfones, photodegradation leading to concomitant loss of physical strength and increased brittleness was brought about by light irradiation at ∼330 nm accompanied by chain scission. The photochemical decomposition of aromatic sulfones and polysulfone occurs from the lowest excited singlet or triplet state via single-photon excitation of ground state molecules. The ablation products of PES observed in this work (Figures 2 and 4) is completely different from the photochemical products observed in the solution; the ablation of PES is not thought to be governed by the photochemical mechanism involving the lowest singlet or triplet state.

Another possible contribution of the photochemical mechanism is from higher excited states based on a multiphoton absorption process of laser pulses. The decomposition of PES from the higher excited states may exhibit analogous fragments observed in Figure 1. However, the ablation products observed significantly differ from the photo fragments in Figure 1 and do not support the decomposition from the higher excited states. Thus the contribution of the decomposition of PES from electronically excited states seems unlikely at least at low fluences of 30−130 mJ/cm^2 used here. Fluorescence spectra from the lowest $\pi-\pi^*$ singlet states of four diaryl sulfones were observed at 280−350 nm at room temperature.[40] The fluorescence lifetimes were 3.2−14.9 ns. If the photochemical mechanism is operative in the ablation of PES, such as the sudden ablation of triazenepolymer,[41] whose etching process was not observed after the end of the laser pulse, the decomposition of PES would be exceptionally fast.

The formation of each product with a certain range of velocity (Figures 3 and 5), the increase in translational energies of C_3H_3 and C_2H_4O with increasing fluence (Figure 6), and the yields of C_3H_3 and $C_{12}H_8SO_2$ obeying a Arrehnius-type law (Figure 7b), as mentioned already, strongly support the dominance of a photothermal mechanism in ablation of PES. The pyrolysis reaction of aromatic sulfones was studied in the gas phase at 500−900 °C.[42] The primary cleavage of the weakest C−S bond, as seen in the photochemical decomposition, was found to occur. The biphenyl with a yield of 10% was produced in the pyrolysis of biphenyl sulfone at 900 °C, although 80% of biphenyl sulfone was recovered. This pyrolysis reaction suggests the occurrence of a thermal decomposition of PES initiated from the breakage of C−S bonds in the chain. From the KL temperature (Figure 10), which indicates a ∼30% lower temperature than that of a laser irradiated surface in the framework of a KL formation model,[18] the temperatures of the laser-irradiated surfaces at fluences of 30−130 mJ/cm^2 can be roughly estimated to be 2500−6100 K.

Although thermal chemistry of sulfones at higher temperatures is not known, unlike the decomposition process of biphenyl sulfone at 900 °C, we propose here the following laser-penetration-depth dependent photothermal ablation model involving a random scission of the PES chain at higher temperatures. First, the absorption of a 266 nm photon to excite each PES molecule to its lowest $\pi-\pi^*$ singlet state is carried out in the chromophores (phenylene rings) of the chain in the film surface. The translational energies up to 24.6 eV obtained for various ablation products (Figure 5) suggest the contribution of multiphotonic absorption[32] during a ns laser pulse. The laser penetration along the depth of the surface brings out the distribution of PES molecules with different degree of excitation in the surface layer.[43] Namely, PES molecules, which absorb more photons, exist at the upper part of the surface layer. The resulting electronic energy is rapidly converted to thermal energy through vibrational relaxation, leading to the formation of a superheated surface layer with temperature gradient along its depth. The estimated temperature of 2500−6100 K depending on the laser fluence probably corresponds to that of the upper surface layer. Subsequently, the decomposition of the PES chain occurs due to breakage of S−C bonds, phenylene rings, etc., resulting in the ejection of the fragments with high translational energies. In this decomposition process, a random scission is expected to occur, while a random scission requires higher activation energy than that of a chain-end-initiated scission. Particularly at the upper part of the surface layer with a higher temperature, drastic chain decomposition into smaller fragments including the cleavage of phenylene rings take place to produce C_3H_3, C_2H_4O, $C_6H_4SO_2$, etc. On the other hand, at the lower part of the surface layer with a lower temperature than that of the upper surface layer, ejection of relatively high-mass fragments to produce $C_{12}H_{10}SO_3$, $C_{13}H_{12}SO_4$, $C_{15}H_{12}SO_4$, etc., occurs with a slightly delayed departure. When the fluence at which ejection of neutral products is dominant is changed, the total amount of the fragments increases due to a deeper penetration depth of laser light. Near the bottom of the surface layer, the decomposition temperature appears to be constant over the laser fluence, resulting in the constant composition of the fragments. This decomposition process is competitive with the dissipation of the thermal energy in the PES chain and thermal diffusion to surrounding PES molecules. Furthermore, the ejection of these gaseous fragments may lead to kick off solid polymeric fragments as seen in ablation of poly(methyl methacrylate)[29,30] and polyimide.[31] Finally, in an adiabatic-like expansion of the fragments in the gas phase, collisions among the fragments bring about the change in their flight velocity distributions and the formation of new products through recombination reactions.

Conclusion

PES films were ablated by 266 nm laser pulses in the fluence region of 30−130 mJ/cm^2. Neutral products arrived at an ion extraction position of a TOF mass spectrometer were detected by delaying a post-ionization laser pulse with respect to an ablation laser pulse. After the investigation of the influence of the post-ionization laser fluence on the detection of neutral products, major ablation products were identified from the peaks in the TOF mass spectra measured for 30 mJ/cm^2. Analysis of the products such as C_3H_3 ($m/e = 39$), $C_6H_4SO_2$ ($m/e = 140$), and $C_{12}H_{10}SO_3$ ($m/e = 234$) indicates that the decomposition of PES occurs due to both the scission of the chain itself and the cleavage of some of the phenylene rings. Arrival dynamics of the neutral products varied product to product. Their average flight velocities ranged from 1.8×10^5 cm/s for $C_{15}H_{12}S_2O_5$ ($m/e = 336$) to 4.1×10^5 cm/s for C_3H_3. In addition, these

products continued to arrive for a period of 6−15 μs, which was over 1200 times the ablation laser pulse length. The change in the composition of the ablation products measured for several higher fluences up to 130 mJ/cm^2 and the flight velocities and the yields of major products as a function of laser fluence were interpreted by the decomposition of the heated surface layer which has a temperature gradient along its depth. From the plots of the yields as a function of fluence, the threshold fluence for neutral fragment ejection was determined to be 10−20 mJ/cm^2. At higher fluences, the yields of neutral products were thought to be affected by the formation of ionic products. Furthermore, the arrival profiles of C_3H_3 at various fluences were found to be narrower than a MB distribution and adequately described by a shifted MB distribution. After the ejection of fragments from the surface, the formation of a KL combined with adiabatic-like expansion is thought to play a significant role. Some of the fragments result in the formation of new recombination products in the expansion process. Finally, we discussed the relevance of photochemical and photothermal mechanisms. The proposed photothermal model, which is laser-penetration-depth dependent and includes random scissions of the polymer chain and cleavage of some phenylene rings, is consistent with our experimental results.

Analysis of the ablation products emerged by laser pulses at low fluences near the ablation threshold did not show any sign of the contribution of the photochemical decomposition of PES. However, under higher intensity laser irradiation, PES may be excited to the higher excited states from which a rapid photochemical decomposition process occurs and becomes a trigger for explosion. Further investigation at higher fluences is required.

References and Notes

(1) Kawamura, Y.; Toyoda, K; Namba, S. *Appl. Phys. Lett.* **1982**, *40*, 374.

(2) Srinivasan, R.; Mayne-Banton, V. *Appl. Phys. Lett.* **1982**, *41*, 576.

(3) Srinivasan, R. In *Laser Ablation-Principles and Applications*; Miller, J. C., Ed.; Springer Series in Materials Sciences 28; Springer-Verlag: Berlin, 1994; p 107.

(4) Bauerle, D. *Laser Processing and Chemistry*; Springer-Verlag: Berlin, 1996; p 191.

(5) Srinivasan, R.; Leigh, W. J. *J. Am. Chem. Soc.* **1982**, *104*, 6784.

(6) Koren, G.; Yeh, J. T. C. *J. Appl. Phys.* **1984**, *58*, 2036.

(7) Brannon, J. H.; Lankard, J. R.; Baise, A. I.; Burns, F.; Kauffman, J. *J. Appl. Phys.* **1985**, *56*, 1984.

(8) Kokai, F.; Koga, Y.; Kakudate, Y.; Kawaguchi, M.; Fujiwara, S.; Kubota, M.; Fukuda, K. *Appl. Phys.* **1994**, *A59*, 299 and references cited therein.

(9) Danilzik, B.; Fabricius, M; Rowekamp, M.; von der Linde, D. *Appl. Phys. Lett.* **1986**, *48*, 212.

(10) Estler, R. C.; Nogar N. S. *Appl. Phys. Lett.* **1986**, *49*, 1175.

(11) Hansen, S. G. *J. Appl. Phys.* **1989**, *66*, 1411.

(12) Otis, C. E. *Appl. Phys.* **1989**, *B49*, 455.

(13) Feldmann, D.; Kutzner, J.; Laukemper, J.; MacRobert, S.; Welge, K. W. *Appl. Phys.* **1987**, *B44*, 81.

(14) Larciprete, R.; Stuke, M. *Appl. Phys.* **1987**, *B42*, 181.

(15) Tsunekawa, M.; Sato, J. *Appl. Phys.* **1989**, *66*, 1411.

(16) Blanchet, G. B.; Fincher Jr, C. R.; Jackson, C. L.; Shah, S. I.; Gardner, K. H. *Science* **1993**, *262*, 719.

(17) Hansen, S. G. *J. Appl. Phys.* **1989**, *66*, 3329.

(18) Kelly, R.; Dreyfus, R. W. *Surf. Sci.* **1988**, *198*, 263.

(19) Kelly, R.; Miotello, A. *Pulsed Laser Deposition of Thin Films*; Chrisey, D. B., Hubler, G. K., Ed.; Wiley: New York, 1994; p 115.

(20) Creasy, W. R.; Brenna, J. T. *Chem. Phys.* **1988**, *126*, 453.

(21) Campbell, E. E. B.; Ulmer, G.; Hasselberger, B.; Busmann, H.-G.; Hertel, I. V. *J. Chem. Phys.* **1990**, *93*, 6900.

(22) Niino, H.; Yabe, A. *Appl. Phys. Lett.* **1989**, *55*, 510.

(23) Niino, H.; Yabe, A. *J. Photochem. Photobiol. A* **1992**, *65*, 303.

(24) Kokai, F.; Koga, Y.; Heimann, R. B. *Appl. Surf. Sci.* **1996**, *96−98*, 261.

(25) Lide, D. R.; Frederikse, H. P. R. *CRC Handbook of Chemistry and Physics*, 76th ed.; CRC Press: Boca Raton, 1985; pp 10−216.

(26) Kokai, F.; Saito, H.; Fujioka, T. *J. Appl. Phys.* **1989**, *66*, 3252.

(27) Kokai, F.; Saito, H.; Fujioka, T. *Macromolecules* **1990**, *23*, 674.

(28) It is not known whether these species are direct fragments from the polymer or reaction products in the gas phase. We therefore ignore the time from laser irradiation to the generation of the fragments or the products.

(29) Srinivasan, R.; Braren, B.; Casey, K. G.; Yeh, M. *Appl. Phys. Lett.* **1989**, *55*, 2790.

(30) Braren, B.; Casey, K. G.; Kelly, R. *Nucl. Instrum. Method B* **1991**, *58*, 463.

(31) Srinivasan, R. *Appl. Phys. A* **1993**, *56*, 417.

(32) Fukumura, H.; Masuhara, H. *Chem. Phys. Lett.* **1994**, *221*, 373.

(33) Srinivasan, R.; Braren, B.; Dreyfus, R. W. *J. Appl. Phys.* **1987**, *61*, 372.

(34) Davis, G. M.; Gower, M. C.; Fotakis, C.; Efthimiopoulos, T.; Argyrakis, P. *Appl. Phys.* **1985**, *A36*, 27.

(35) Zhigilei, L. V.; Kodali, P. B. S.; Garrison, B. J. *J. Phys. Chem.* **1998**, *102*, 2845.

(36) Dickinson, J. T.; Shin, J. J.; Langford, S. C. *Appl. Surf. Sci.* **1996**, *96−98*, 326.

(37) Khrasch, N.; Khodair, A. I. A. *Chem. Comm.* **1967**, 98.

(38) Nakai, M.; Furukawa, N.; Oae, S. *Bull. Chem. Soc. Jpn.* **1972**, *45*, 1117.

(39) Randy, B.; Rabek, J. F. *Photodegradation, Photooxidation and Photostabilization of Polymers*; John Wiley: New York, 1975; p 223.

(40) Abdul-Rasoul, F.; Cateral, C. L. R.; Hargreaves, J. S.; Mellor, J. M.; Phillips, D. *Eur. Polym. J.* **1977**, *13*, 1019.

(41) Lippert, T.; Stebani, J.; Ihlemann, J.; Nuyken, O.; Wokaum, A. *J. Phys. Chem.* **1993**, *97*,12296.

(42) Davis, F. A.; Panunto, T. W.; Awad, S. B.; Billmers, R. L. *J. Org. Chem.* **1984**, *49*, 1228.

(43) The measurement of etch depths after laser irradiation at 4×10^{-5} Pa was performed separately using a mechanical stylus (Rank Taylor Hobson Talystep). The etch depths per laser pulse were 30−250 nm at 30−130 mJ/cm^2 estimated by the depths of the holes made by 30−200 laser shots.